Energy Conversion System based on Photovoltaic-Battery-Ultra Capacitor-Diesel Sources for a Mobile Hospital

Mohamed Zine Zizoui
Ecole Militaire Polytechnique
bekheira tabbache (laid_tabache@yahoo.com)
Ecole Militaire Polytechnique https://orcid.org/0000-0002-0940-1834
Muhammad Fahad Zia
Brest University: Universite de Bretagne Occidentale
Mohamed Benbouzid
Brest University: Universite de Bretagne Occidentale

Research

Keywords: Photovoltaic Generator, Battery, Ultra-capacitor, Diesel generator, Energy Management, Mobil Hospital, VOC

Posted Date: September 29th, 2021

DOI: https://doi.org/10.21203/rs.3.rs-889228/v1

Abstract

This article deals with the energy management of a hybrid system composed of PV, Battery,ultracapacitor and diesel synchronous generators for a mobile hospital. The proposed power system can supply energy to Shelter Hospital for better treatment of patients in remote states, particularly in the event of a pandemic situation such as COVID-19. For this reason, a hybrid power system in which a diesel generator is used with a photovoltaic energy source for reliable availability of power supply. Moreover, batteries and ultra-capacitors are also integrated to obtain a hybrid power generation and storage system to ensure the smooth operation of mobile hospital weather conditions. Photovoltaic panels are connected to a boost converter to follow maximum power tracking (MPPT) and Power curtailment modes. The battery is connected to a bidirectional reversible DC-DC converter for DC bus voltage regulation and state of charge (SOC) control. The ultra-capacitor is associated with the battery to compensate for the peak power. The diesel generator is connected in parallel with the photovoltaic generator, battery, and ultra-capacitor to continuously provide the power required by the load. The integrated operation of all the generation and storage systems is complex for shelter hospital. Hence; an efficient energy management algorithm is developed to manage the continuous energy flow between the elements of the hybrid power system and mobile hospital load through the control of the power converters.

Finally, validation results are presented to show the effectiveness of the proposed energy management of the hybrid power system.

1. Introduction

In remote areas and particularly in the sub-Saharan territories, the low population distribution has led to difficulties in ensuring on-site health coverage in urgent cases requiring medical evacuation, such as the Covid-19 pandemic [1, 2]. For this reason, it is suggested that mobile hospitals be built or deployed in the desert and remote areas. This type of hospital includes several modules of treatment and diagnostic equipment to adapt to any emergency [3]. These medical modules require a continuous power supply from diesel generators that suffer from high fuel costs and preventive maintenance [4].

For this reason, in remote areas with high solar potential, the combination of a diesel generator with photovoltaic generators offers a better quality of service to reduce operating costs and allow the successful gradual transition from fossil to renewable sources [5, 6]. To increase efficiency, excess energy from diesel and PV generators needs to be stored using storage systems. For some industrial applications requiring high peak power, batteries suffer from short mass life at high energy (5–10 years) [7] and low dynamic behavior. However, peak power can be supported by ultra-capacitors which are characterized by high power density and low voltage devices [8, 9], and therefore this technology represents a major challenge in determining the relationship between energy production and consumption in a mobile hospital. In this context, there is an insufficient number of research studies that address this problem except for the few studies that concern large hospitals [10], which is conducting an in-depth study to be able to determine this relationship, for [11], which illustrates the profile of electrical

energy consumption in an isolated hotel where its consumption is pre-dimensioned according to the number of clients or visits during the year. On the other hand, [12] has proposed a model for distributing the energy produced between the different departments of a hospital while minimizing the energy cost, and in the same context [13] has proposed works that can increase the resilience of a hospital powered by renewable energy and a conventional source such as a diesel generator by optimizing the dimensions of its components, all these studies do not cover the case of a mobile hospital or its dimensioning depends on the circumstances and locations of crises.

The integration of different production and storage systems for mobile hospitals requires an efficient management strategy. In this context, many papers have proposed applications studied in micro networks that are designed for autonomous operation, where the main control objective is to know how to manage the energy flow between the different loads of the system.

In the micro-grid framework, the literature deals with many control strategies. For a PV-diesel stand-alone hybrid power system, a control approach has been presented in [14] which present experimental results of a PV-diesel hybrid system without storage. These results show the radiation relationship and the load profile for a good sizing of this system that can cause the diesel generator to operate around its rated power which should be equal to the peak load. In [39], presents a frequency sharing approach to mitigate the effect of weather or sea state variations on the integrated micro-grid on board a ship. A hybrid storage system based on ultra-capacitor and battery is developed such that high power and short-term fluctuations are handled by the ultra-capacitor and batteries. In [34], proposes a method for controlling the power balance of a multi-source micro-grid hybrid system to meet the DC load power demand with reliability and DC bus voltage stabilization. In the same context, [38] proposes a coupling structure of the DG on the DC bus side to slow down the power dynamics produced by the DG, which will be imposed by the inverter and ensure the efficiency and profitability of the system by operating the DG around its rated power, on the other hand [36] proposes a voltage and frequency control strategy for a system with high intermittent renewable power generation.

In this case, an energy storage system has been connected to the AC bus via an inverter instead of a DG, the storage is used to generate the nominal frequency, which makes the system frequency independent of the mechanical inertia of a synchronous generator.

Most of the energy management techniques presented above require the DG to be kept operational often to avoid transition regimes of operating modes. Indeed, in [35] and [37], a transition control strategy between the connected and disconnected modes of the grid was proposed for a three-phase voltage source based on the calculation of reference powers and a virtual impedance control strategy to achieve efficient power distribution in the hybrid energy storage elements, where the battery provides steady-state power and supports only transient power fluctuations respectively or the synchronization problem has been well studied in both modes. In [38], a clear control methodology for the transition between the different modes was developed.

In this context, this paper proposes a new energy flow supervision for a PV-Diesel-HESS micro-grid that takes into account optimized management in different operating modes. Consequently, the PV panels are coupled to a boost converter at maximum power and power limiting (Off-MPPT). Also, the batteries are connected to a reversible DC-DC converter to regulate the terminal voltage (DC bus terminals) and control the state of charge (SOC). The ultra-capacitor is associated with the batteries to compensate for peak power. The diesel generator is connected in parallel with the photovoltaic generator (photovoltaic, batteries, and ultra-capacitor) to provide the insufficient power required by the load. In this context, an algorithm is developed to manage the energy flow between the hybrid power elements and the load through the control of the power converters.

2. Power Sizing Of The Mobile Hospital

List of medical and non-medical equipment with their estimated daily energy needs according to their power consumption priority in Table (1):

Table 1 Estimated daily energy of medical and non-medical equipment

Basic equipment						
Equipment	Power (W)	Hours used per day (h)	Energy per day (Wh/day)	First Priority	Second Priority	Third Priority
Lights (fluorescent)	11	8	90	x		
Mobile phone charger	5-20	8	40-160			x
Ceiling fan (CD, AC)	30-100	8	300-800			x
Water pump	100	8	600	x		
Computer	15-200	4.5	67.5-900		x	
Portable electrical heater	1000-1500	2	2000-3000			x
Radio	2-30	8	16-240			x
Printer (ink, laser)	65-1000	2	130-1000		x	
Small waste autoclave	600-6000	1	600-3000			x
Medical equipment						
Sterilizer (steam)	500-1560	2	1000–3200			x
Suction	24	10	240		x	
Pulse Oximetry	24	3	72	x		
Reverse-osmosis Water purifier	260-570	7	1820–2590	x		
X-ray machine (dental)	200	1	200	x		
X-ray machine (portable and fixed)	300-11000	2	600–4000	x		
Mechanical ventilator	608	3	1824		x	
Ultrasound scanner	75	2-3	150–225	x		
Electrocardiogram (ECG)	50-80	1	50–80		x	
Nebulizer	180	3-5	540–900			x
Laboratory equipment						
Vaccine refrigerator (165 L)	40-500	4	160–2000	x		
Microscopes	30	2	60		x	
Centrifuge	600	3	900		x	
Spectrophotometer	63	1	68			
Blood chemistry analyzer	45	2	90	x		
Hematology Analyzer	230	2	460		x	
Arterial blood gas (ABG) analyzer	250	0.5	125	x		

During the design, the sizing of the power appears as an important aspect. It must be done in such a way as to ensure a continuous power supply while ensuring energy availability at a lower cost. The sizing depends on both the meteorological characteristics depending on the location and the required load demand. Or the 24 h load profile is shown in Fgure (1)

3. System Structure Hybrid System

Figure 2 shows the parallel hybrid system. It is composed of a photovoltaic generator as renewable energy, batteries, ultra-capacitor, diesel generator as a source of emergency energy, and power electronics converters as elements of electric power exchange of energy flow in the system.

The PV generator is associated with the boost converter to extract the maximum power. The batteries and the Ultra-capacitor are connected to a reversible DC-DC converter. The diesel generator is connected in parallel with the DC bus using a bidirectional inverter while it is directly connected with the AC load.

3.1 PV generator

In photovoltaic cells are based on pure Silicon with certain chemical elements [15, 16].

Photovoltaic cells are mounted in series or in parallel on solar PV modules to obtain a voltage suitable for electrical applications. The panels require solar energy to transform into DC electrical energy, which can be either directly fed to loads or stored in batteries [17, 18]. Hence, the number of cells in the PV module depends on the required power.

The equivalent electrical circuit of the solar cell is presented in Fig. 2 [19, 20].

By applying the Kirchhoff law:

Ipv = I_{ph} - I_d - I_p (1)

For photovoltaic generator composed of «N_s» serial panels and «N_p» parallel panels, the characteristic current-voltage relation is given by:

$$I_{PV} = N_p I_{ph} - N_p I_0 \left(e^{\left(\frac{V_{PV} + R_{sG} I}{N_s a V_T} \right)} - 1 \right) - \frac{V_{PV} + R_{sG} I_{PV}}{R_{pG}}$$

2

$$R_{sG} = \frac{N_s R_s}{N_p}, R_{pG} = \frac{N_s R_p}{N_p}$$

Where:

V_{pv} : is Panel voltage (V). I_{ph} :is Photocurrent (A)and I_{pv} :is Panel current (A). Ion : is Saturation current. q: is Coulomb constant (1.602e-19C) and k : is Boltzmann's constant (1.38 e-23 [J/K]). R_s : is Series cell resistance (Ω) and R_p : is Parallel cell resistance (Ω). G: is Global insulation (W/m2).

3.2 Batteries

Different battery models are presented in the literature. A battery model of Figure (3) consists of an ideal battery, presented by a voltage source E_o and an internal resistance R_{bat} [20, 21].

The voltage between batteries is expressed by:

$$\mathrm{V_{bat}} = \mathrm{E_0} - (\mathrm{R_{bat}} \times \mathrm{i_{bat}}) - \mathrm{Vc_{bat}}$$

03

The state of charge (SOC) is given by

$$\mathrm{Soc_{bat}} = (1 - \frac{\mathrm{Q_d}}{\mathrm{C_{bat}}}) \times 100\backslash\%$$

04

Where:

Q_d is the nominal capacity of the battery in (Ah) and C_{bat} is the missing quantity of charge about Q_d.

3.3 Ultra-capacitor

The ultra-capacitor model is composed of equivalent serial resistance (R_{es}), equivalent parallel resistance (R_{ep}), and capacitor (C_{uc}) [22, 23].

The SOC of ultra-capacitor is expressed as a function of the voltage at the terminals of the ultra-capacitors according to the relation:

$$\mathrm{SOC_{uc}} = \frac{\mathrm{V_{uc}}}{\mathrm{V_{nom-uc}}}$$

5

With V_{nom-uc}: Nominal Voltage of the Load.

3.4 Diesel generator modeling

The diesel generator is composed of a diesel engine, a synchronous generator, and the excitation system as shown in Figure (5) [24, 25].

Where:

The DG torque model is based on expression (6)

$$\mathrm{T_{mec}} = \phi\,(\mathrm{s})\,\mathrm{e}^{-\mathrm{s}\tau_1}$$

6

The mechanical equation is written as

$$\frac{\mathrm{d}\Omega}{\mathrm{dt}} = \frac{1}{\mathrm{J_T}}(\mathrm{T_{mec}} - \mathrm{T_e} - \mathrm{D_T}\Omega)$$

7

$$\phi\,(\mathrm{s}) = \frac{\mathrm{ka}}{1 + \mathrm{s}\tau_2}\mathrm{C}$$

8

φ(s): is the fuel flow adjusted by the governor and the motor torque.

4. Power Management Of The Hybrid System

4.1 Generator control

The PV generator is connected to a voltage boost converter to adapt the PV output to the DC bus. Also, this converter extracts the maximum power from the PV generator. The following figure illustrates the scheme of the PV system managed by two different types the MPPT-based Perturb and Observe and Curtailment Power (Off-MPPT) algorithm.

The DC-DC boost converter can be modeled by the following relationship:

$$\begin{cases} \frac{\mathrm{di_L}}{\mathrm{dt}} = \frac{1}{\mathrm{L}}(-\,(1+\mathrm{d})\,\mathrm{V_{dc}} + \mathrm{V_{pv}}) \\ \frac{\mathrm{dV_{pv}}}{\mathrm{dt}} = \frac{1}{\mathrm{C_{pv}}}(\mathrm{i_{pv}} - \mathrm{i_L}) \end{cases}$$

9

For the maximum power point tracking (MPPT)], the Perturb and Observe (P&O) method are widely adopted regarding their effectiveness and simplest implementation with minimum measurement inputs [26, 27, 28]. It is based on the measurement of the voltage and current inputs of the PV generator. By using perturbation to the input voltage, changes can be observed in the power output to provide the next control sequence of the boost converter. If electrical power increases, the disturbance should continue in the same direction. Otherwise, the disturbance direction will be inversed. Figures (7.a) shows the (P&O) strategy scheme.

4.2 .DC bus control

DC Bus control contains mainly battery, ultra-capacitors, and two bi-directional DC/DC converters. As shown in Fig. 7, battery and ultra-capacitors are connected to bidirectional dc-dc converters. The power

management between the battery and the ultra capacitor's storage system is ensured by the frequency separation controller.

Both storage elements (batteries and ultra-capacitors) can be operated in two modes: charging and discharging modes.

The bidirectional DC-DC converter of the battery can be modeled by:

$$\frac{\mathrm{di_{bat}}}{\mathrm{dt}} = \frac{1}{\mathrm{L}}[(\alpha_{\mathrm{bat}})\,\mathrm{V_{dc}} - \mathrm{V_{bat}})]$$

10

The bidirectional DC-DC converter of the ultra-capacitors can be modeled by:

$$\frac{\mathrm{di_{uc}}}{\mathrm{dt}} = \frac{1}{\mathrm{L}}[(\alpha_{\mathrm{uc}})\,\mathrm{V_{dc}} - \mathrm{V_{uc}})]$$

11

To regulate the DC bus voltage by the frequency separation technique, the storage elements should provide currents equal to the common current I_L.

After the Low-Pass Filter (LPF) of the current reference, the high-frequency component of the DC bus passed by the ultra-capacitor and the low frequency through a battery. In this way, the battery current reference ($I_{Lbat-ref}$) can be obtained and the reference current of the ultra-capacitor ($I_{Luc-ref}$) is obtained by the difference between the two currents (I_{L-ref} and $I_{Lbat-ref}$).

In figure (8), the DC bus voltage is coordinately controlled by the battery and ultra capacitor sources. The DC bus voltage U_{dc} is compared with the reference DC bus voltage $_{Udc-ref}$, the difference presents the input of the proportional- integration (PI) controller which provides the current reference I_{ref}.

4.3 AC bus control

Two operating modes (connected or disconnected from the (DG) for the AC bus are detailed as follows:

1.1 Disconnected-Grid Mode (Off-Grid)

In this mode, the system is disconnected from the diesel engine. So, the Diesel engine disconnected from the AC bus. The purpose of this mode is to control the inverter to provide an AC voltage with regulated amplitude and frequency based on the dq- frame technique. For this, the voltage across the filter capacitor should be regulated which the voltage reference contains non-zero frequencies. This method provides good control performance and protects against overloads and short circuits. [29, 30–31].

This type of technique is shown in Fig. 9, where L_f, R_f, and C_f are respectively the inductor, the internal resistance of the inductor, and the capacitor of the LC filter, V_{dc} represents the regulated voltage at the input of The regulated voltage across the capacitor is the voltage supplied to the three-phase load. The

switching method is based on pulse width modulation (SVM). The differential equations describing the dynamics of the inverter can be derived as follows:

$$\mathrm{V}_{\mathrm{inv,abc}} = mV_{dc} = R_f I_{L,abc} + L_f \frac{dI_{L,abc}}{dt} + V_{abc}$$

12

$$I_{L,abc} = C_f \frac{dV_{abc}}{dt} + I_{Load,abc}$$

13

$$\begin{bmatrix} \mathrm{V_d} \\ \mathrm{V_q} \end{bmatrix} = \frac{1}{CS} \begin{bmatrix} (Cw)\, V_q \\ -(Cw)\, V_d \end{bmatrix} + \frac{1}{CS} \begin{bmatrix} I_{Ld} - I_{Load-d} \\ I_{Lq} - I_{Load-q} \end{bmatrix}$$

14

$$\begin{bmatrix} I_{Ld} \\ I_{Lq} \end{bmatrix} = \frac{1}{L_f S + R_f} \begin{bmatrix} V_{id} - V_d \\ V_{iq} - V_q \end{bmatrix} + \frac{1}{L_f S + R_f} \begin{bmatrix} \left(L_f w\right) I_{Lq} \\ -\left(L_f w\right) I_{Ld} \end{bmatrix}$$

15

Where:

$V_{inv,abc}$: is the three-phase inverter output voltage, m: is the three-phase control signals, V_{abc}: is the three-phase filter capacitor output voltage, and $I_{Load,abc}$: is the three-phase load output current.

2.1 Grid -Connected Mode

In this mode, the Diesel engine is connected with the AC bus. In this case, the DC bus voltage is connected to the AC bus via a bidirectional inverter with an LC filter.

Thus, the diesel generator can operate in parallel with the inverter by synchronizing the output voltages. For this, to estimate the AC angular frequency, a phase-locked loop (PLL) should be included in the control system.

The power inverter control is based on the Voltage Orientation Control (VOC) using the instantaneous powers (active and reactive) and the output voltage of the diesel generator [32, 33]. Shown by the following equations:

The voltage across the filter (LC) is given by:

$$V_{an} = L_f \frac{di_{Lf}}{dt} + R_f i_{Lf} + V_{cf}$$

16
In a diesel generator connected mode, the V_{cf} =0

$$V_{an} + \mathrm{V_{DG,a}} = L_f \frac{di_{Lf}}{dt} + R_f i_{Lf}$$

17

$$I_{Load,abc} = I_{DG,abc} + I_f$$

18
The conventional convergence of a mathematical model of a stationary coordinate system with the synchronous rotary two-phase coordinate system (dq) presented according to the following equations

$$\begin{cases} V_D = L_f \frac{d\mathrm{I_D}}{dt} + R_f I_D - L_f w I_Q + E_D \\ V_Q = L_f \frac{d\mathrm{I_Q}}{dt} + R_f I_Q + L_f w I_Q + E_Q \end{cases}$$

19

$$\begin{cases} L_f \frac{d\mathrm{I_d}}{dt} + R_f I_D = \left(K_p + \frac{K_i}{S}\right) \times \left(I_{d-ref} - I_D\right) \\ L_f \frac{d\mathrm{I_Q}}{dt} + R_f I_Q = \left(K_p + \frac{K_i}{S}\right) \times \left(I_{q-ref} - I_Q\right) \end{cases}$$

20
From (19) and (20) the final expression is given by:

$$\begin{cases} V_{d-rf} = \left(K_p + \frac{K_i}{S}\right) \times \left(I_{d-ref} - I_D\right) - L_f w I_Q + E_D \\ V_{q-ref} = \left(K_p + \frac{K_i}{S}\right) \times \left(I_{q-ref} - I_Q\right) + L_f w I_Q + E_Q \end{cases}$$

21

5. The Proposed Management Algorithm

The management and sharing of power in the different parts of the electrical system are developed according to the state of charge and discharge of the storage element (battery). In this case, the ultra-capacitor state of charge is kept between 97.4% and 98.4%].

According to this algorithm, there are seven (7) operating modes of this system which are Table (1):

5.1 Diesel engine Disconnected Mode (DEDM)

This mode is activated when battery SOC is greater than 25% (SOC_{bat}> 25%). In this case, the PV generator operates either in MPPT mode or in Off-MPPT (Power Curtailment). Therefore, it has two sub-modes:

5.1.1 Power Curtailment Mode (PCM)

This operating mode is selected when the power of the photovoltaic generator meets the total load demand and the two (02) storage elements are fully charged i.e. (Socbat > 90%), The PV power must be limited to a reference value lower than Pmpp (Maximum PowerPoint).

The control algorithm enabling PC is represented in the flowchart given in Fig. (7.b).

5.1.2 Maximum Power Point Tracking Mode (MPPTM)

This mode is activated when the state of charge of the battery-less than the maximum permissible state (90 < SOC_{bat}> 25%). In this case, the PV generator operates in MPPT mode to extract the maximum amount of electrical energy depending on the climatic conditions. The storage elements have the possibility of absorbing or compensating to keep the DC bus around its value of reference Vdc_ref = 700V, the diesel generator is stopped and all loads are connected.

5.2 Diesel Engine Connected Mode (DECM)

This mode is selected when the state of charge of the battery pack is equal to 25%. In this case, the diesel generator operates at its nominal power in parallel with the PV in MPPT mode and charges the storage elements up to 90%.

5.3 First Priority Load Mode (FPLM)

When the diesel generator is operating alone and the state of charge of the batteries and the ultra-capacitors is insufficient and continues to charge (weak climatic conditions) below 10%, the system will be unable to satisfy the main load (load P_1). In this case, the load must be disconnected to allow the hybrid storage device to charge.

5.4 Second Priority Load Mode (SPLM)

If the state of charge of the hybrid storage is between 10% and 15% (10% <SOCbat ≤ 15%), the load with the second priority (load P_2) will be disconnected and only the load with the priority (load P_1) will remain connected.

5.5 Third Priority Load Mode (TPLM)

This mode is activated when the operation of the diesel generator is connected and when the state of charge of the batteries is below 20% but remains above 15%. To avoid an additional discharge of the batteries, the supervision algorithm will disconnect the load with the lowest priority (P_3).

The following table summarizes the different operating modes of the studied system :

Table 2
Different operating modes of the studied system

		Different Operating Mode						
N°	State of Hybrid Storage Element (%)	PCM	MPPTM	DEDM	DECM	FPLM	SPLM	TPLM
01	Soc_{bat}> 90%	1	0	1	0	1	1	1
02	90% < Soc_{bat} > 25%	0	1	1	0	1	1	1
03	25% < Soc_{bat} > 15%	0	1	0	1	1	1	0
04	15% < Soc_{bat} > 10%	0	1	0	1	1	0	0
05	Soc_{bat} < 10%	0	1	0	1	0	0	0

6. Validation Result And Discussion

To validate the power management algorithm mentioned above, the following parameters are used:

Table 3
PV generator Parameters

PVGenerator reference	DC converter
BPSolar SX3190	L_{pv} :5mH
N_s : 16, Np :6	C_{pv} :5µF
P_n :260,43	

Table 4
DC System Parameters

Lead acid battery	DC converter	UC	DC converter	DCBus
250v,40AH	L_{bat}= 4mH	5F ,R_{uc}= 8,9Mω	L_{uc}=5mH	V_{dcRef}=700v,C_{bus}=2mF
τ_{bat} = 1.5s		V_{uc}= 215v		

Table 5
AC Source Parameters

Diesel Engine Parameters	Filter Parameters
P_n=20KW,w_n=1500rpm,τ_1 = 0.01s,τ_2 = 0.02s	R_f=2.66Ω,L_f=47Mh,
K = 40,Torque Limits [0 1.1]	Cf = 100µF
	Ts = 5e-5,F_s=5Kh

Table 6
Controller Parameters of the different modes connection

Disconnected mode	Connected mode
PLL K_p=0.2325,K_i= 5.254	PLL K_p=0.1114,K_i= 3.3416
Filter K_p=1.200, K_i=300.251	Filter K_p=1.1000,K_i=136.7273

Figure (15) shows the illumination profile used in the simulation.

The DC bus voltage, presented in figure (16), is followed by its reference (700V) after a response time until the connection of the diesel engine. To regulate (decrease) the voltage Vdc, the inverter intervenes by absorbing the surplus current to inject it into the storage sources and discharge the ultra-capacitor until Vdc = 700V.

Figure (17) Fig. (18) shows the operation of the hybrid system according to the proposed management algorithm.

Noted that the DC sources quickly meet the system requirements in terms of power demand in both DC and AC bus. The appearance of different operating modes of the system starting with the MPPT mode at 0.10 sec.

When the Ppv > Pload, the extraction of the active power given by the photovoltaic generator supplied the power requested by the load and the surplus will be transported to the storage bench (charge the Batteries and ultra capacitors).

After the drop in the lighting profile and the increase in the load (G = 700V/m^2, P = 25kW) the diesel group intervenes and the mode DECM is activated to ensure the maximum of power supplied to the load and the batteries. At the instant 25 Sec, the storage systems are sufficiently charged and the power requested by the load is sufficient which leads to the appearance of the mode PCM until the moment 40 sec and limits the power generated by the PV. At the instant 40 sec and after a slight disturbance, the MPPT mode is activated again and the batteries begin to recharge.

Figure 21 illustrates the two operating modes of the proposed systems (disconnected mode and connected mode). The specified mode appears between 0.10 sec and 25.50sec when the active power is requested (Pload < Pdc). Between 10sec and 25sec], the diesel engine intervenes to ensure the power requested by the load in the connected mode.

Figure 22 shows the two connections of the inverter and the diesel engine with disturbances due to the synchronization of the two voltage sources in the two operating modes. Due to the starting of the diesel

engine, the alternative voltage is provided by the inverter (disconnected mode) until 13sec when the engine diesel stabilizes.

The battery and ultra capacitor (SOC) level given in Figs. 23 and 24 respectively are shows the reliability of the management algorithm.

7. Conclusion

In this paper, a multi-source system (PV generator–batteries–ultra-capacitor and diesel generator) has been presented. For this, an effective management algorithm is developed to improve system efficiency and optimize energy consumption. So, the DC bus can be controlled by a storage system presented by batteries and ultra-capacitors, and the AC bus can be controlled by two different methods namely dq frame and voltage oriented control depending on the operating mode. In this context, the DC bus is regulated using the frequency separation controller, in which both storage systems can operate in charge and discharge modes. On the other hand, the AC bus is controlled by two techniques mentioned above in which these two techniques have proven their effectiveness in terms of control and management in a system with different types of power sources and according to the required load profile.

Declarations

Availability of data and materials: All data generated or analyzed during this study are examined by our group and certified for several times.

Competing interests : The authors declare they have no competing interests.

Funding : Not applicable.

Authors' contributions : Mohamed Zine Zizoui provided real test data, Bekheïra Tabbache supported the test data and wrote the paper, Muhammad Fahad Zia analyzed the test data, and Mohamed Benbouzid organized the researched full structure. All authors read and approved the final manuscript.

Acknowledgements : Not applicable.

References

[1] Ouma O P, Maina J, Thuranira P N, Macharia P M, Alegana VA, English M, Okiro E A, Snow R W. Access to emergency hospital care provided by the public sector in sub-Saharan Africa in 2015: a geo coded inventory and spatial analysis. The lancet Global Helth .2018; 6(3): 342-350.

[2] Juran S, Broer P N, Klug S J, Snow R C, Okiro E A, Ouma P O ,Snow R W, Tatem A J, Meara J G, Alegana V A. Geospatial mapping of access to timely essential surgery in sub-Saharan Africa. BMJ Glob Health.

2018;3:1-10.

[3] Bakowski J. A Mobil Hospital – Its Advantages and Functional Limitations. Int. J. of Safety and Security Eng .2016; 6, 4: 746–754.

[4] Issa M,Ibrahim H , Hosni H ,Ilinca A, Rezkallah M. Effects of Low Charge and Environmental Conditions on Diesel Generators Operation. Eng .2020; 1:137-152.

[5] Aussela D, Neveua P, Tsuanyoa D, Azoumah Y.On the equivalence and comparison of economic criteria for energy projects: Application on PV/diesel hybrid system optimal design. Energy Conversion and Management .2018;163 : 493-506.

[6] Costa T S, Villalva M G.Technical Evaluation of a PV-Diesel Hybrid System with Energy Storage: Case Study in the Tapajós-Arapiuns Extractive Reserve, Amazon, Brazil. Energies. 2020; 13: 2969.

[7] Sabihuddin S, Kiprakis A E, Mueller M. A Numerical and Graphical Review of Energy Storage Technologies. Energies. 1996;1073:172-216.

[8] Haidl P, BuchroithnerA, SchweighoferB, BaderM, WegleiterH. Lifetime Analysis of Energy Storage Systems for Sustainable Transportation. Sustainability. 2019; 11, 6731:1-21.

[9]Agbli K S , Hilairet M , Gustin F .Real-Time Control Based on a CAN-Bus of Hybrid Electrical Systems Rea.Energies. 2020;13, 4502:1-14.

[10] Gonzáleza A G, Calcedob J G S, Salgadoc D R. A quantitative analysis of final energy consumption in hospitals in Spain.2018;169-175.

[11] Mohamed M A , M.Eltamaly A, Alolah A I.Sizing and techno-economic analysis of stand-alone hybrid photovoltaic-wind-diesel- battery power generation systems.Journal of Renewable and Sustainable Energy .2015; 77, 063128 .

[12] Syed M I, Chem Nayar V, Mubashwar Hasan M. Power Electronics for Renewable Energy Sources.Science Direct, Power Electronics Handbook, Fourth Edition.2018; 783-827.

[13] Alexis Lagrangea,b, Miguel de Simón-Martínb,, Alberto González-Martínezb, Stefano Braccoc, Enrique Rosales-Asensiob. Sustainable microgrids with energy storage as a means to increase power resilience in critical facilities: An application to a hospital.Electrical Power and Energy Systems. 2020; 19; 105865.

[14] Mutarraf M U,TerricheY , Niazi K A K ,Khan F, Vasquez JC, Guerrero JM. Control of Hybrid Diesel/PV/Battery/Ultra-Capacitor Systems for Future Shipboard Microgrids. Energies .2019;12(18), 3460.

[15] Klugmann-Radziemska E, Ostrowski P. Chemical treatment of crystalline silicon solar cells as a method of recovering pure silicon from photovoltaic modules. Renewable Energy .2010;35:1751–1759.

[16] Huang WH,Shin WJ, Wang L , Wen Cheng S ,Tao M. Strategy and technology to recycle wafer-silicon solar modules. Solar Energy .2017; 144: 22–31.

[17]Nayak P K, Mahesh S, Snaith H J, Cahen, D. Photovoltaic solar cell technologies: analyzing the state of the art.Nature Reviews Materials . 2019;4:269–285.

[18]K.H. Tang, K.H. Chao, Y.W. Chao, J.P. Chen, .Design and Implementation of a Simulator for Photovoltaic Modules, International Journal of Photonergy. 2012.

[19] Widyolar B, Jiang L, Brinkley J, Hota S K, Ferry J, Diaz G, Winston R. Experimental performance of an ultra-low-cost solar photovoltaic-thermal (PVT) collector using aluminum minichannels and nonimaging optics.2020;268, 114894.

[20]Sarita K, Devarapalli R, Rai P. Modeling and control of dynamic battery storage system used in a hybrid grid. Energy Storage. 2020;2:e146.

[21] Li Y , Vilathgamuwa M , Farrell T , Choi SC, Ngoc Tham Tran a , Joseph Teague. A physics-based distributed-parameter equivalent circuit model for lithium-ion batteries. Electrochimica Acta. 2019;299: 451-469.

[22] Logerais PO, Camara M A , Riou O, Djellad A , Omeiri A , Delaleux F , Durastanti JF. Modeling of a supercapacitor with a multibranch circuit. International Journal of Hydrogen Energy.2015;40(39): 13725-13736.

[23] Helseth L E.Modeling supercapacitors using a dynamic equivalent circuit with a distribution of relaxation times.Journal of Energy Storage. 2019; 25, 100912.

[24] Sakamoto O. An example of a diesel generator model with fluctuating engine torque for transient analysis using XTAP. Journal of International Council on Electrical Engineering .2016;6;1: 31-35.

[25] Mishra S, Ramasubramanian D. Improving the Small Signal Stability of a PV-DE-Dynamic Load-Based Microgrid Using an Auxiliary Signal in the PV Control Loop.IEEE Trans. Power Syst. 2016; 30:166–176.

[26] Christopher I.W., Ramesh R.,. Comparative Study of P&O and InC MPPT Algorithms. American Journal of Engineering Research (AJER), e-ISSN: 2320-0847 p-ISSN: 2320-0936 Volume-02, Issue-12:402-408.

[27] Jose A. Carrasco J A , Garcia de Quiros F, Alaves H, Navalon M. An Analog Maximum Power Point Tracker With Pulse width Modulator Multiplication for a Solar Array Regulator. IEEE Transactions On Power Electronics. 2019;39(4):8808 – 8815.

[28] Bhattacharyya S, Dattu Sampath K, Samanta S, Mishra S. Steady Output and Fast Tracking MPPT (SOFT-MPPT) for P&O and InC Algorithms. IEEE Transactions on Sustainable Energy. 2021;12(1): 293 -

302.

[29]TaoY,LiuQ, DengY, Liu X,He X. Analysis and Mitigation of Inverter Output Impedance Impacts for Distributed Energy Resource Interface. IEEE Transactions on Power Electronics.2015;30(7): 3563- 3576.

[30] Ramezani M, Li S, SunY. DQ-reference-frame based impedance and power control design of islanded parallel voltage source converters for integration of distributed energy resources.Electric Power Systems Research. 2019;168:67–80.

[31]Kosari M, Hosseinian S H.Decentralized Reactive Power Sharing and Frequency Restoration in Islanded Microgrid. IEEE Transactions on Power Systems.2016;32(4): 2901 - 2912.

[32] Mazhar SM, Haq U,Tulasi Ram S S, Subramanyam J B V. Voltage Oriented Control(VOC) Of The PWM Rectifier Using Active Filtering Function.International Journal of Engineering & Technology. 2018; 7 (2.19) : 90-93.

[33] Zamani M H , Riahy G H , Abedi M. Rotor-Speed Stability Improvement of Dual Stator-Winding Induction Generator-based Wind farms By Control-Windings Voltage Oriented Control. IEEE Transactions on Power Electronics.2015;31(8): 5538 – 5546.

[34] Changjie Yin, Hongwei Wu, Fabrice Locment, Manuela Sechilariu. Energy management of DC microgrid based on photovoltaic combined with diesel generator and supercapacitor. Energy Conversion and Management. 2017; 132; 14-27.

[35]Choudar A,Boukhetela D,Baraket S,Brucker JM. A local energy management of a hybrid *PV*- storage based distributed generation for microgrids. Energy Conversion and Management. 2015; 90 :21-33.

[36] Yun-Su Kim, Eung-Sang Kim,Seung-Il Moon.Frequency and Voltage Control Strategy of Standalone Microgrids With High Penetration of Intermittent Renewable Generation Systems, IEEE Transactions on Power Systems.2016;vol31,issue1 ; 718 – 728.

[37] Wen S, Wang S, Liu G. Energy Management and Coordinated Control Strategy of PV/HESS AC Microgrid During Islanded Operation .IEEE Access. 2018;Vol7: 4432 – 4441.

[38]Gassab S,Radjeai H, Mekhilef S,Adel Coudar A. Power management and coordinated control of standalone active PV generator for isolated agriculture area-case study in the South of Algeria. Renewable Sustainable Energy.2018; 11; 015305.

[39] Mutarraf MU , Yacine Terriche Y , Niazi KAK , han F , Vasquez JC , GuerreroJM. Control of Hybrid Diesel/PV/Battery/Ultra-Capacitor Systems for Future Shipboard Microgrids. Energies .2019; 12, 3460:1-22.

Figures

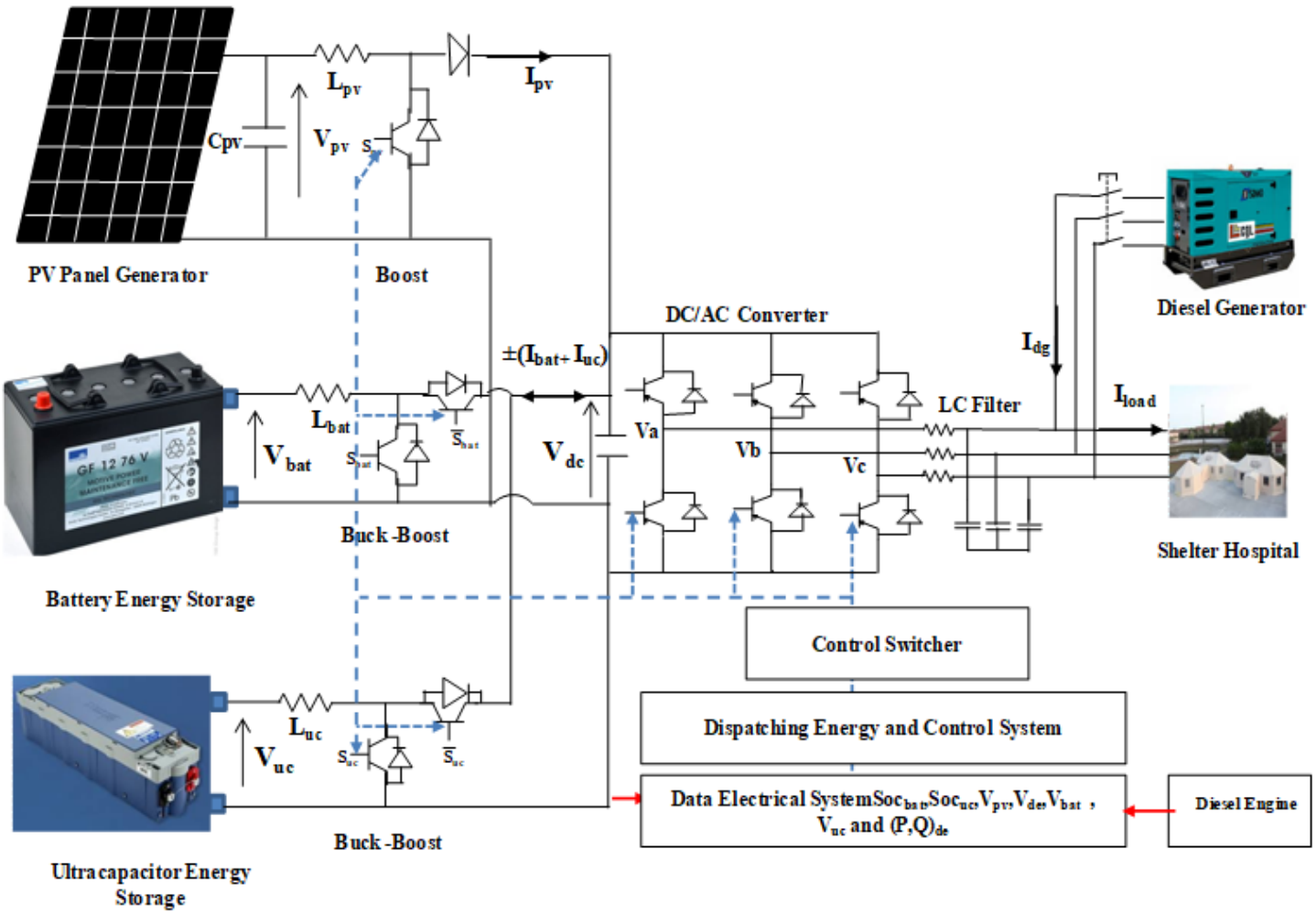

Figure 2

Parallel Hybrid system structure

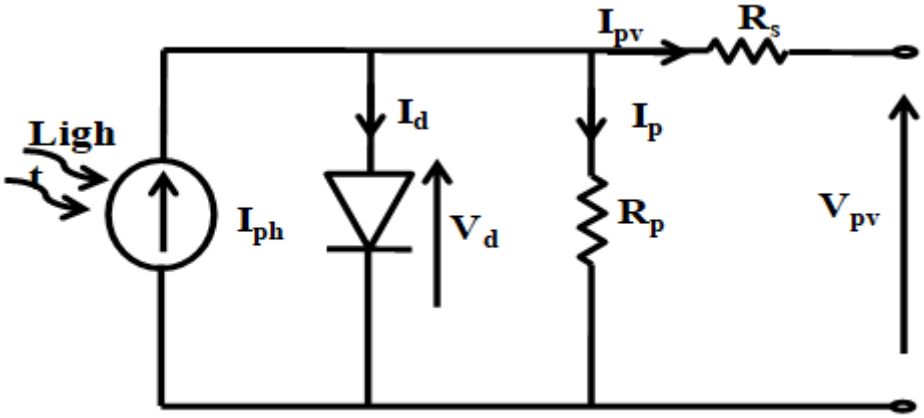

Figure 3

Solar cell model.

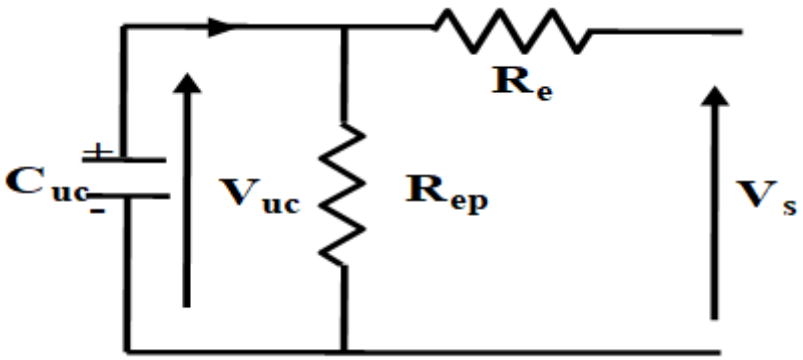

Figure 5

Ultra-capacitor model.

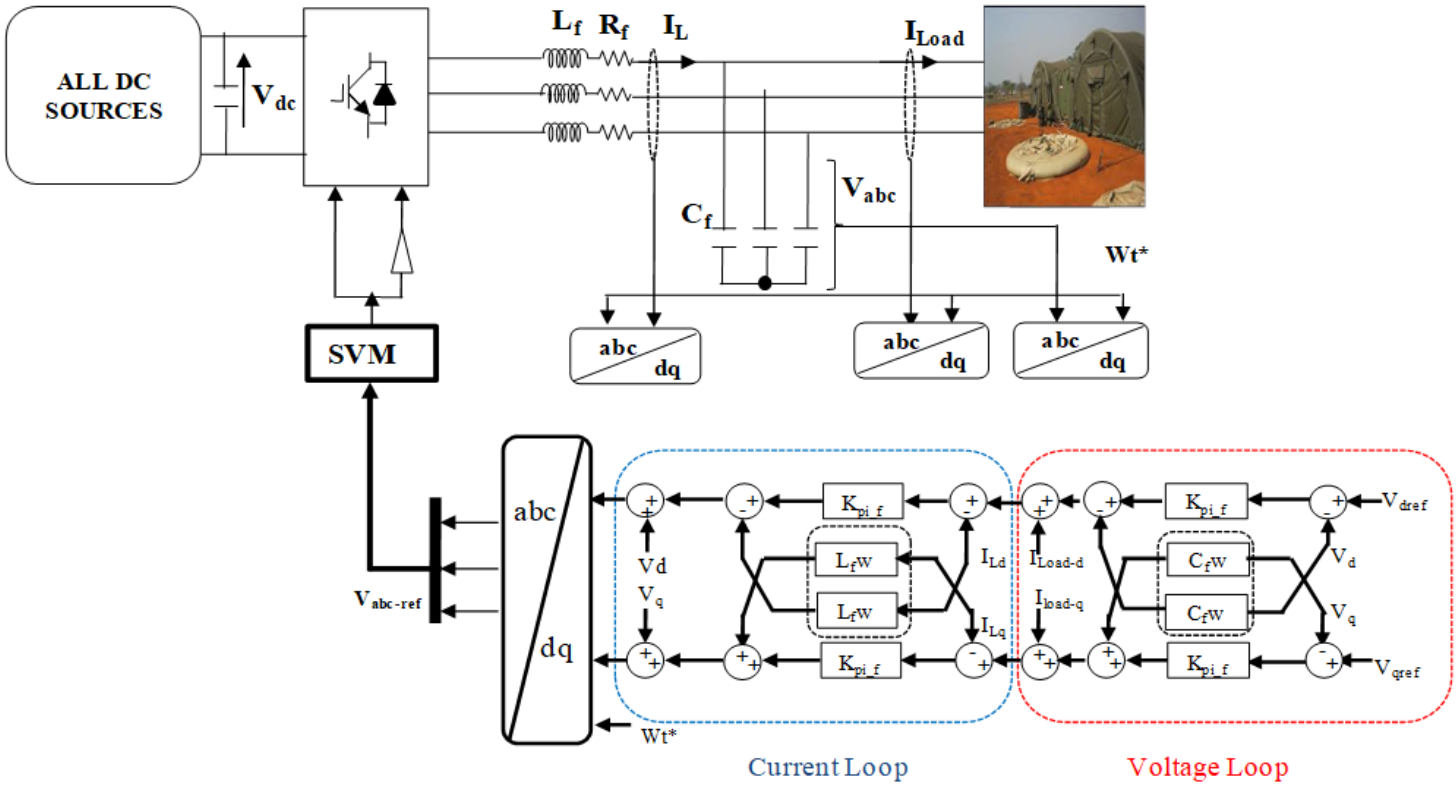

Figure 11

DQ Frame Technique Controller

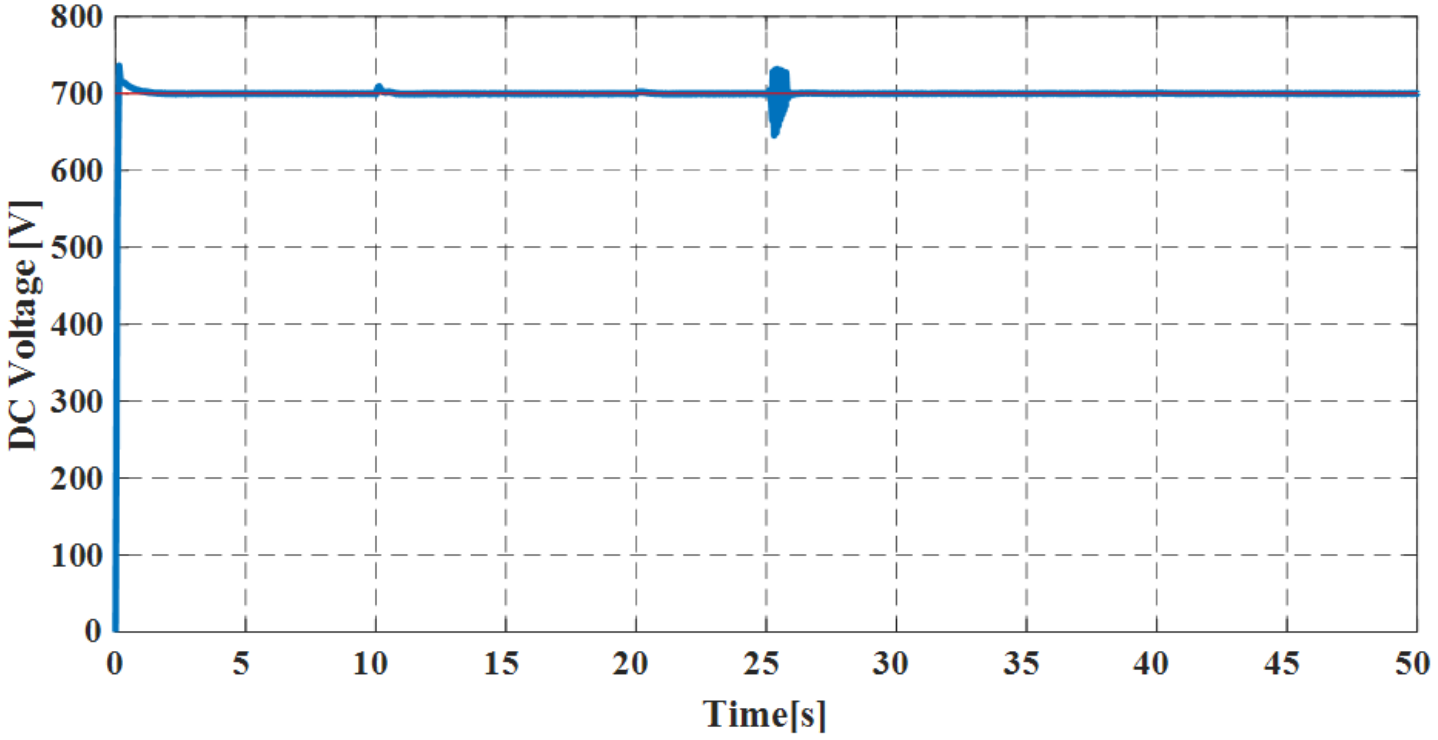

Figure 17

DC Bus Voltage (V)

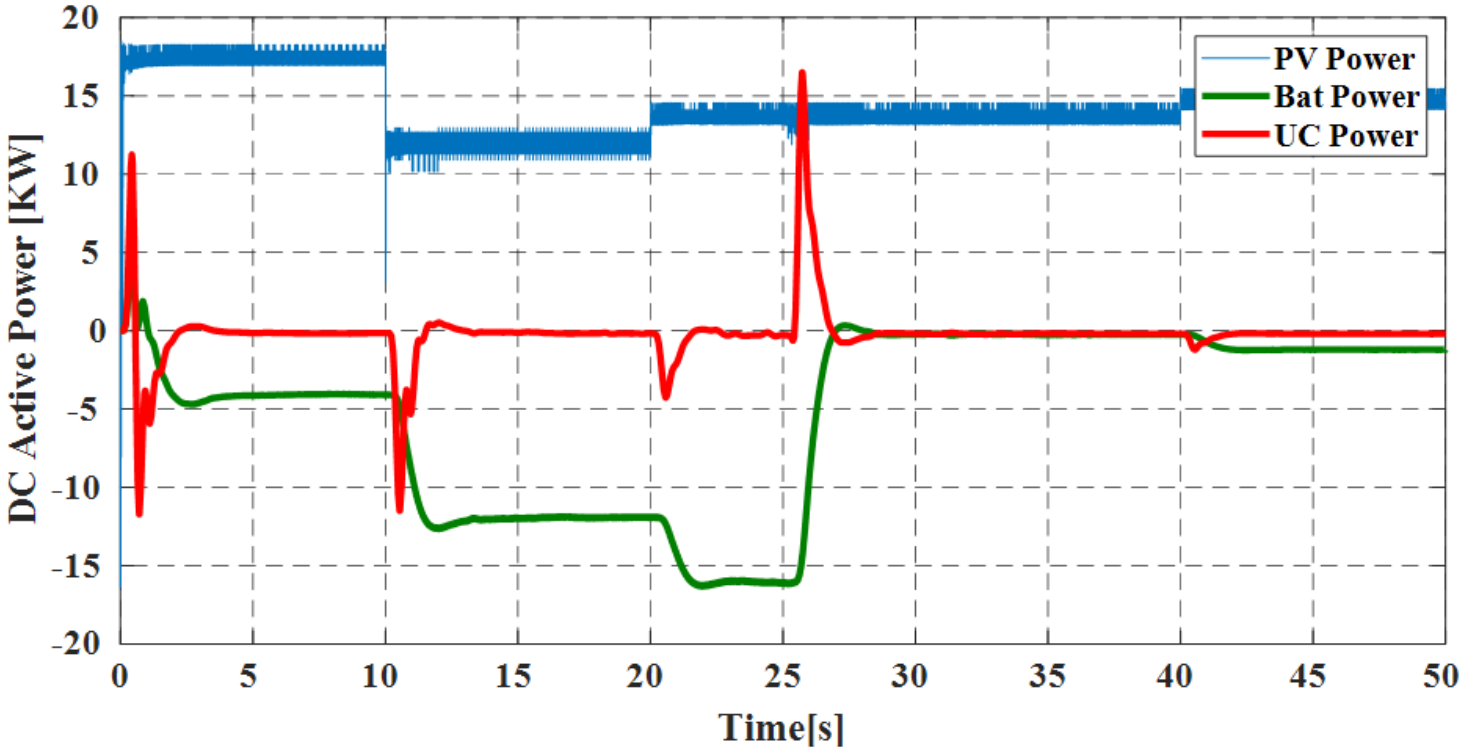

Figure 18

Power Responses: PV Power (Blue), Batteries Power (Green), and UC Power (Red)

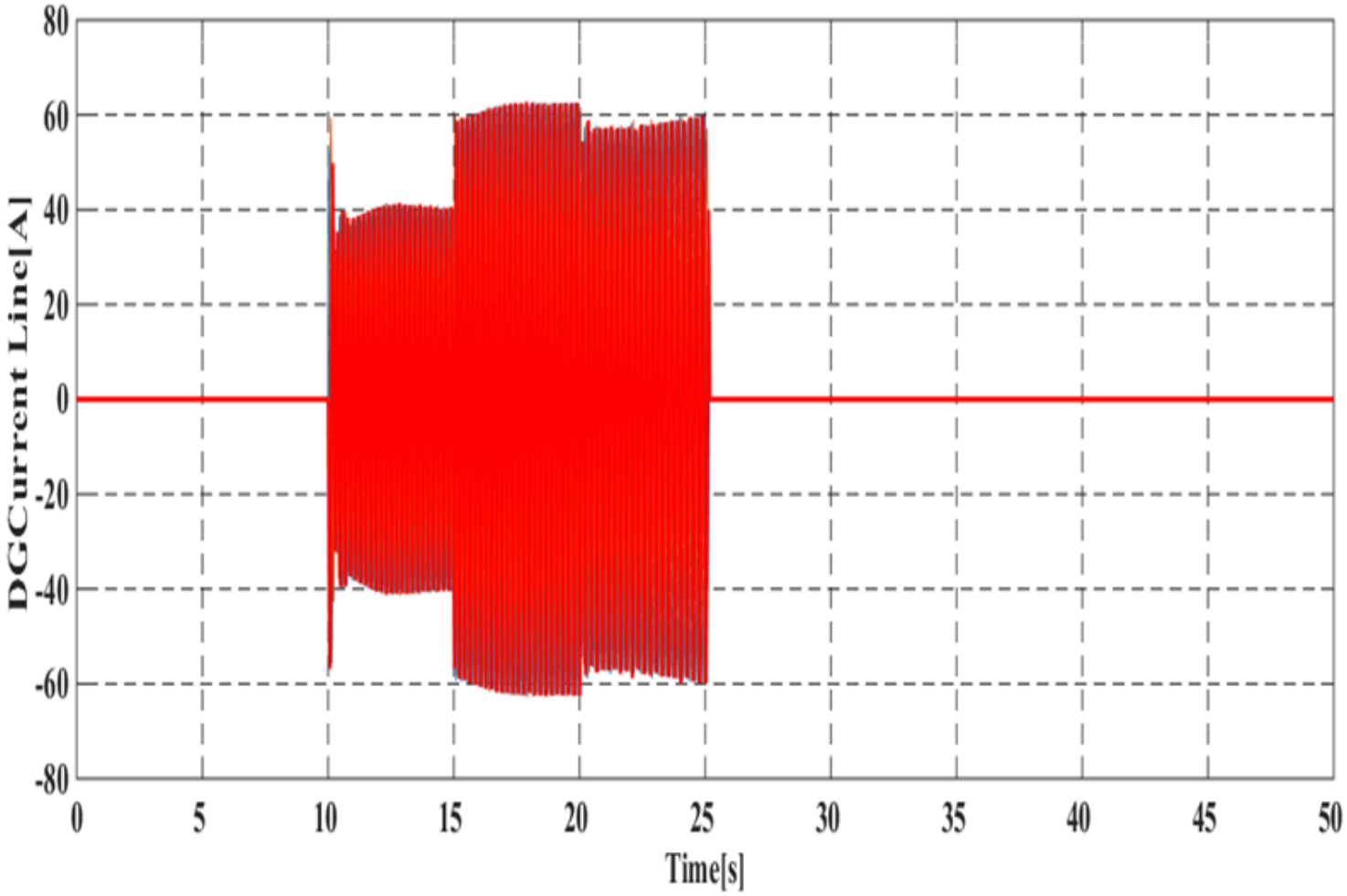

Figure 21

Diesel Engine Current (A)

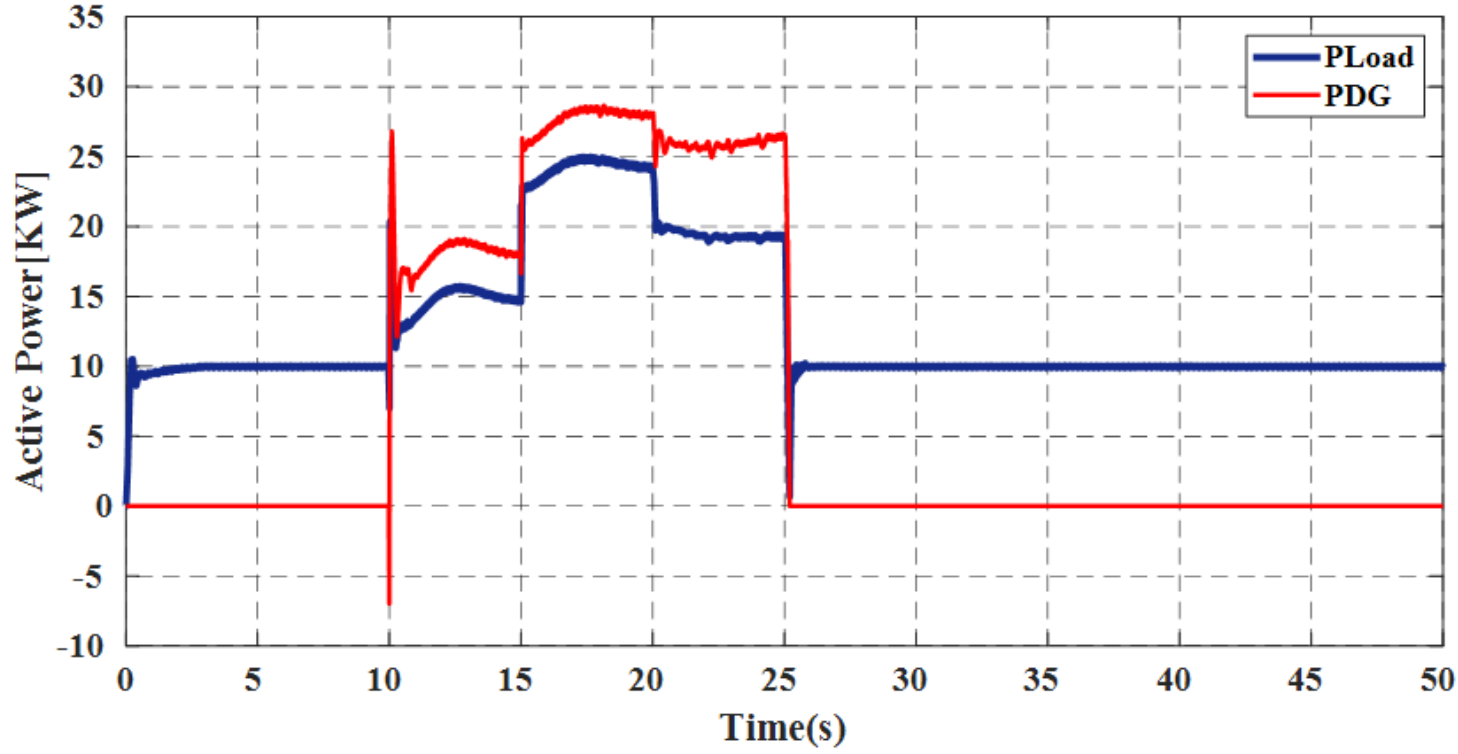

Figure 22

AC power Load (Bleu), Diesel Engine (Red)